Available online at http://scik.org
J. Math. Comput. Sci. 10 (2020), No. 2, 277-288
https://doi.org/10.28919/jmcs/4367
ISSN: 1927-5307

PERISTALTIC TRANSPORT OF CONDUCTING WILLIAMSON FLUID IN A POROUS CHANNEL

B. REDDAPPA[1,*], A. PARANDHAMA[1], S. SREENADH[2]

[1]Department of BS & H, Sree Vidyanikethan Engineering College, Tirupati-517102, India

[2]Department of Mathematics, Sri Venkateswara University, Tirupati-517502, India

Abstract. In physiology, peristalsis is used to transport the biofluid from a region of lower pressure to higher pressure in the living body. Most of the biofluids (such as blood) are classified as non-Newtonian fluids. In some pathological conditions, the distribution of fatty cholesterol and artery clogging blood clots in the lumen of coronary artery can be modeled as fluid flow in a porous tube. In view of this, the peristaltic flow of a conducting non-Newtonian Williamson fluid in a porous channel with flexible walls under the effects of radiation is investigated. The problem is solved applying perturbation method. Velocity distribution and pressure flow characteristics are calculated and the effects of various emerging parameters on the flow characteristics are discussed in detail.

Keywords: peristalsis; Williamson fluid; MHD; porous medium.

2010 AMS Subject Classification: 35Q35.

1. INTRODUCTION

In mammals, an important mechanism namely, peristalsis is observed by medical doctors Bayliss and Starling [1]. Since this phenomenon is necessary for life of humans and animals, several investigators are carried out by engineers and mathematicians all over the world [2–14]. This biofluid principle is applied by biomedical and mechanical engineers in the design of peristaltic pumps and medical devices such as heart lung machine. Preliminary experimental study is done by Latham [15]. The theoretical work of Jaffrin and Shapiro [16] made a land mark

*Corresponding author
E-mail address: drbreddappa@gmail.com
Received November 13, 2019

in the biological study of peristalsis. The study on peristaltic flow pertaining Newtonian fluid with different geometries is thoroughly investigated by researchers like Vajravelu *et al* [17, 18], Subba Reddy *et al* [19]. As the walls of the biological ducts (for example blood vessel) are composed of tissues surrounding the biofluids, the impact of bounded porous medium came into existence an according Vajravelu [20, 21, 22] did commendable work to explain the significance of the bounding layers.

Peristaltic motion in a two-dimensional uniform channel with a long wave using sinusoidal wave approximation of an incompressible non-Newtonian Carreau fluid through a porous medium is studied El Shehawey *et al*. [23]. The effect of induced magnetic field on pulsatile fluid of peristaltic flow through porous medium bounded by a 2-D channel was analyzed Afifi and Gad [24] and they are observed that the high permeability parameter and no magnetic field ($K \to \infty$, $M \to 0$) our result is in agreement with the existing results. Mekheimer and Arabi [25] analyzed the characteristics of peristaltic transport of electrically conducting viscous fluid flow through a porous medium. El Shehawey [26] analyzed the incompressible viscous fluid flow of a peristaltic transport through a porous medium with asymmetric channel. Navaneeswar Reddy and Viswanatha Reddy [27] have discussed the slip effects on peristaltic motion of a williamson fluid through a porous medium in a planar channel. Abdulhadi and Ahmed [28] have studied the effect of magnetic field on peristaltic flow of Williamson fluid through a porous medium in an inclined tapered asymmetric channel. Mishra and Ramachandra Rao [29] studied peristaltic transport of a Newtonian fluid in a two-dimensional asymmetric channel under the assumptions of long wavelength and low Reynolds number in a wave frame of reference. Ali et al. [30] have investigated peristaltic flow of MHD fluid in a channel with variable viscosity under the effect of slip condition.

In view of these, we studied the Peristaltic transport of conducting Williamson fluid in a planar channel, under the assumptions of low Reynolds number and long wavelength. The channel is bounded by permeable layers. The flow is investigated in a wave frame of reference moving with velocity of the wave. The perturbation series in the Weissenberg number ($We < 1$) was used to obtain explicit forms for velocity field, pressure gradient and friction force per one wavelength. The effects of Weissenberg number We, Darcy number Da, amplitude ratio ϕ, Hartmann number M and slip parameter α on the pumping characteristics are discussed through graphs in detail.

2. MATHEMATICAL FORMULATION

We consider the peristaltic motion of a conducting Williamson fluid through a porous medium in a two-dimensional symmetric channel of width $2a$. The flow is generated by sinusoidal wave trains propagating with constant speed c along the channel walls. A rectangular co-ordinate system (X, Y) is chosen such that X-axis lies along the centre line of the channel in the direction of wave propagation and Y-axis transverse to it. The fluid flow in the channel is bounded by permeable layers. In the permeable layers the flow is governed by Darcy's law. Fig.1 depicts the physical model of the problem. The wall deformation is given by

$$Y = \pm H(X,t) = \pm a \pm b \sin \frac{2\pi}{\lambda}(\mathrm{X} - \mathrm{ct}) \tag{1}$$

where b is the wave amplitude, λ is the wave length, and X, Y are the rectangular co-ordinates with X measured along the channel and Y perpendicular to c is the velocity of propagation and x is the direction of wave propagation X.

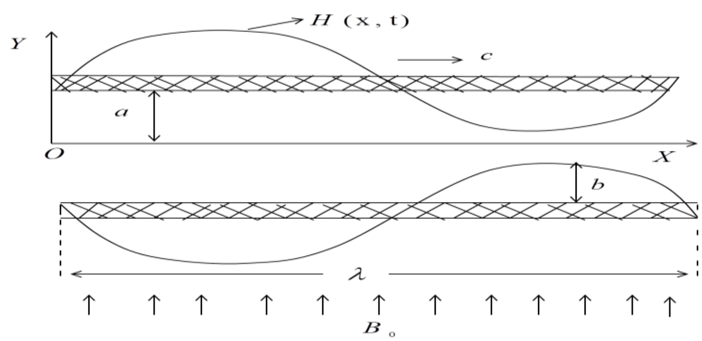

Fig.1. The Physical Model

A uniform magnetic field of strength B_0 is applied in the transverse direction to the flow. The induced magnetic field is neglected by assuming small magnetic Reynolds number. The electric field is taken zero. Under the assumptions that the channel length is an integral multiple of the wave length λ and the pressure difference across the ends of the channel is a constant, the flow becomes unsteady in the laboratory frame (X, Y). However, in a co-ordinate system moving with the propagation velocity c (wave frame (x, y)), the boundary shape is stationary. The transformation from fixed frame to wave frame is given by

$$x = X - ct,\ y = Y,\ u = U - c,\ v = V,\ p(x) = \mathrm{P}(X,t) \tag{2}$$

where U and V are velocity components in the laboratory frame and u and v are velocity components in the wave frame, p and P are the pressures in wave and fixed frames of reference respectively.

The equations governing the flow in a wave frame are

$$\frac{\partial u}{\partial x}+\frac{\partial v}{\partial y}=0 \tag{3}$$

$$\rho\left(\frac{\partial u}{\partial x}+\frac{\partial v}{\partial y}\right)=-\frac{\partial p}{\partial x}-\frac{\partial \tau_{xx}}{\partial x}-\frac{\partial \tau_{yx}}{\partial y}-\sigma B_0^2(u+c) \tag{4}$$

where ρ is the density, p is the pressure and σ is the electrical conductivity.

Introducing the non-dimensional quantities

$$\bar{x}=\frac{x}{\lambda},\ \bar{y}=\frac{y}{a},\ \bar{u}=\frac{u}{c},\ \bar{v}=\frac{v}{c\delta},\ \delta=\frac{a}{\lambda},\ \bar{p}=\frac{pa^2}{\eta_0 c\lambda},\ h=\frac{H}{a},\ \bar{t}=\frac{ct}{\lambda},\ \bar{\tau}_{xx}=\frac{\lambda}{\eta_0 c}\tau_{xx},$$

$$\bar{\tau}_{yx}=\frac{a}{\eta_0 c}\tau_{yx},\ Re=\frac{\rho ac}{\eta_0},\ We=\frac{\Gamma c}{a},\bar{q}=\frac{q}{ac},\ M=\sqrt{\frac{\sigma}{\eta_0}}aB_0 \tag{5}$$

Using the above non-dimensional quantities and the resulting equations in terms of velocity function can be written as

$$\frac{\partial u}{\partial x}+\frac{\partial v}{\partial y}=0 \tag{6}$$

$$Re\,\delta\left(u\frac{\partial u}{\partial x}+v\frac{\partial u}{\partial y}\right)=-\frac{\partial p}{\partial x}-\delta^2\frac{\partial \tau_{xx}}{\partial x}-\frac{\partial \tau_{yx}}{\partial y}-M^2(u+1) \tag{7}$$

where δ, Re, We, M represent the wave, Reynolds, Weissenberg and Hartmann numbers respectively. Under the assumption of long wave length and low Reynolds number, neglecting the terms of order δ and Re, we get

$$\frac{\partial p}{\partial x}=\frac{\partial}{\partial y}\left[\left(1+We\left(\frac{\partial u}{\partial y}\right)\right)\frac{\partial u}{\partial y}\right]-M^2(u+1) \tag{8}$$

Here p is a function of x only. So that Eq. (8) can be rewritten as

$$\frac{dp}{dx}=\frac{\partial^2 u}{\partial y^2}+We\,\frac{\partial}{\partial y}\left[\left(\frac{\partial u}{\partial y}\right)^2\right]-M^2(u+1) \tag{9}$$

The corresponding dimensionless boundary conditions are

$$\frac{\partial u}{\partial y}=0 \quad \text{at} \quad y=0 \tag{10}$$

$$u=-1-\frac{\sqrt{Da}}{\alpha}\,\frac{\partial u}{\partial y} \quad \text{at} \quad y=h \tag{11}$$

The non dimensional volume flow rate q in a wave frame of reference is given by

$$q = \int_0^h u\, dy \tag{12}$$

$$Q(X,t) = \int_0^H U\, dy = \int_0^h (u+1)\, dy = q + h \tag{13}$$

The time averaged flux over one period $T\left(= \lambda/c\right)$ of the peristaltic wave is

$$\overline{Q} = \frac{1}{T}\int_0^T Q dt = \int_0^1 \left(q+h\right) dx = q+1 \tag{14}$$

3. SOLUTION

We seek for a regular perturbation in terms of small parameter We as follows

$$u = u_0 + We\, u_1 + O(We^2) \tag{15}$$

$$\frac{dp}{dx} = \frac{dp_0}{dx} + We\, \frac{dp_1}{dx} + O(We^2) \tag{16}$$

$$q = q_0 + We\, q_1 + O(We^2) \tag{17}$$

Substituting these equations into the equations (9), (10) and (11), we get

3.1. SYSTEM OF ORDER ZERO

$$\frac{dp_0}{dx} = \frac{\partial^2 u_0}{\partial y^2} - M^2 (u_0 + 1) \tag{18}$$

with the boundary conditions

$$\frac{\partial u_0}{\partial y} = 0 \ \text{ at } \ y = 0 \tag{19}$$

$$u_0 = -1 - \frac{\sqrt{Da}}{\alpha}\frac{\partial u_0}{\partial y} \ \text{ at } \ y = h \tag{20}$$

3.2. SYSTEM OF ORDER ONE

$$\frac{dp_1}{dx} = \frac{\partial^2 u_1}{\partial y^2} + \frac{\partial}{\partial y}\left[\left(\frac{\partial u_0}{\partial y}\right)^2\right] - M^2 u_1 \tag{21}$$

with the boundary conditions

$$\frac{\partial u_1}{\partial y} = 0 \text{ at } y = 0 \tag{22}$$

$$u_1 = -\frac{\sqrt{Da}}{\alpha}\frac{\partial u_1}{\partial y} \text{ at } y = h \tag{23}$$

3.3. SOLUTION OF ORDER ZERO

Solving Eq. (18) using the boundary conditions (19) and (20), we get

$$u_0 = \left(\frac{dp_0}{dx}\right)\left[\frac{\cosh My}{M^2 A_1} - \frac{1}{M^2}\right] - 1 \tag{24}$$

The volume flow rate q_0 is given by

$$q_0 = \left(\frac{dp_0}{dx}\right)\left[\frac{\sinh Mh}{M^3 A_1} - \frac{h}{M^2}\right] - h \tag{25}$$

From Eq. (25), we have $\frac{dp_0}{dx} = \frac{q_0 + h}{A_{10}}$ (26)

3.4. SOLUTION OF ORDER ONE

Substituting Eq. (24) in Eq. (21) and solving it using the boundary conditions (22) and (23), we get

$$u_1 = A_{11}\cosh My + A_{12}\sinh My - \frac{1}{M^2}\frac{dp_1}{dx} - \frac{A_2^2}{3}\sinh 2My \tag{27}$$

The volume flow rate q_1 is given by

$$q_1 = A_{10}\left(\frac{dp_1}{dx}\right) + A_2^2 A_7 \tag{28}$$

From Equations (28) and (26) we have

$$\frac{dp_1}{dx} = \frac{q_1 - A_2^2 A_7}{A_{10}} \tag{29}$$

$$\frac{dp}{dx} = \frac{(q+h)}{A_{10}} - We\frac{(q_0+h)^2 A_7}{A_{10}^3 M^4 A_1^2} \tag{30}$$

The dimensionless pressure rise per one wavelength in the wave frame is defined as

$$\Delta p = \int_0^1 \frac{dp}{dx}\,dx \tag{31}$$

APPENDIX:

$$A_1 = \cosh Mh + \frac{\sqrt{Da}}{\alpha} M \sinh Mh, \quad A_2 = \left(\frac{dp_0}{dx}\right)\left[\frac{1}{\left(M^2 A_1\right)}\right], \; A_{11} = \frac{\left(\frac{1}{M^2}\right)\left(\frac{dp_1}{dx}\right) + A_2^2 A_7}{A_1}, \; A_{12} = \frac{2A_2^2}{3}$$

$$A_3 = \sinh 2Mh - 2\sinh Mh - \frac{\sqrt{Da}}{\alpha} 2M\left(\cosh Mh - \cosh 2Mh\right), \quad A_4 = A_1 \sinh Mh, \quad A_5 = \frac{A_4}{A_1},$$

$$A_6 = -2\cosh Mh + \frac{\cosh 2Mh}{2} + 3, \quad A_7 = \frac{\left(A_5 + A_6\right)}{3M}, \quad \mathrm{A}_8 = \frac{\sinh Mh}{M^3 A_1}, \quad A_9 = \frac{h}{M^2}, \quad A_{10} = A_8 - A_9 .$$

4. RESULTS AND DISCUSSION

In order to obtain the physical insight of the problem, the variation of pressure gradient, pressure rise are computed numerically for different values of the emerging parameters, viz., Weissenberg number We, Darcy number Da, Hartmann number M using MATLAB package and are presented in Figures 2-11.

Fig. 2 shows the variation of pressure gradient $\frac{dp}{dx}$ for different values We with $\phi = 0.5,\ Da = 0.1,\ M = 1,\ q = -1$ and $\alpha = 0.3$. It is observed that the variation of axial pressure gradient $\frac{dp}{dx}$ enhances with rising We. Fig. 3 depicts the variation of pressure gradient $\frac{dp}{dx}$ for different values Da with $\phi = 0.5, We = 0.01,\ \mathrm{M} = 1,\ q = -1$ and $\alpha = 0.3$. It is noted that the variation of axial pressure gradient $\frac{dp}{dx}$ diminishes with rising Da. Fig. 4 shows the variation of axial pressure gradient $\frac{dp}{dx}$ for different values of ϕ with $We = 0.01,\ Da = 0.1,$ $M = 1,\ q = -1$ and $\alpha = 0.3$. It is found that the variation of axial pressure gradient $\frac{dp}{dx}$ enhances with rising ϕ except at the end of the channel. Fig. 5 shows the variation of pressure gradient $\frac{dp}{dx}$ for different values M with $We = 0.01,\ Da = 0.1,\ \phi = 0.5,\ q = -1$ and $\alpha = 0.3$. It is observed that the variation of axial pressure gradient $\frac{dp}{dx}$ enhances with rising M. Fig. 6 shows the variation of pressure gradient $\frac{dp}{dx}$ for different values α with. $We = 0.01,\ Da = 0.1,$ $\phi = 0.5,\ q = -1$ and $M = 1$. It is observed that the variation of axial pressure gradient $\frac{dp}{dx}$ enhances with rising α.

Fig. 7 presents the variation of pressure rise Δp with $\bar{Q}$ for different values of We with $We = 0.01, \phi = 0.5, M = 1$ and α=0.1 . It is observed that the average volume flow rate $\bar{Q}$ enhances with an rising in We in all the three regions; viz., pumping ($\Delta p > 0$), free-pumping ($\Delta p = 0$) and co-pumping ($\Delta p < 0$) regions. Fig. 8 shows the variation of pressure rise Δp with $\bar{Q}$ for different values of Darcy number Da with $We = 0.01, \phi = 0.5, M = 1$ and α=0.1. It is found that any two curves intersecting in first quadrant to the left of the point of intersection, the $\bar{Q}$ diminishes with rising Da whereas to the right of this point of intersection $\bar{Q}$ enhances with rising Da . Fig. 9 presents the variation of pressure rise Δp with $\bar{Q}$ for different values of amplitude ratio ϕ with $We = 0.01, Da = 0.1, M = 1$ and α=0.1 . It is observed that the $\bar{Q}$ enhances with increasing ϕ both in the pumping and free-pumping regions, whereas it diminishes with rising ϕ in the co-pumping region for chosen ($\Delta p < 0$). The variation of pressure rise Δp with $\bar{Q}$ for different values of Hartmann number M with $We = 0.01, Da = 0.1, \phi = 0.5$ and α=0.1 is shown in Fig. 10. It is noted that, any two pumping curves intersect in the first quadrant. To the left of this point, the $\bar{Q}$ enhances and to the right of this point it diminishes with rising Hartmann number M . Fig. 11 illustrates the variation of pressure rise Δp with $\bar{Q}$ for different values of slip parameter α with $We = 0.01, Da = 0.1, \phi = 0.5$ and $M = 1$ It is found that the $\bar{Q}$ enhances with rising α in both the pumping region and free pumping region. An interesting observation is that in the co-pumping region, as α enhances $\bar{Q}$ diminishes in the co-pumping region for chosen ($\Delta p < 0$).

5. CONCLUSIONS

In peristaltic transport of a Williamson liquid, the impact of pertinent physical parameters occurred in the problem is studied on the pumping characteristics. Some of the interesting pumping characteristics are given below:

- The pressure gradient in the flow and the average flux diminishes with rising Darcy number.
- The pressure gradient in the flow and the average flux enhances with rising Hartmann number.
- The pressure gradient in the flow and the average flux enhances with rising slip parameter.
- The pressure gradient in the flow and the average flux enhances with rising Amplitude ratio.

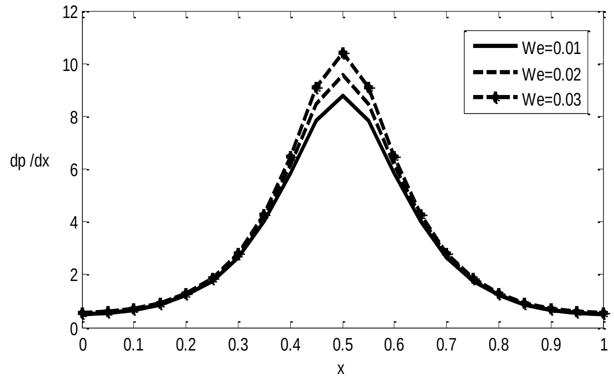

Fig. 2. The variation of axial pressure gradient $\frac{dp}{dx}$ for different values of We.

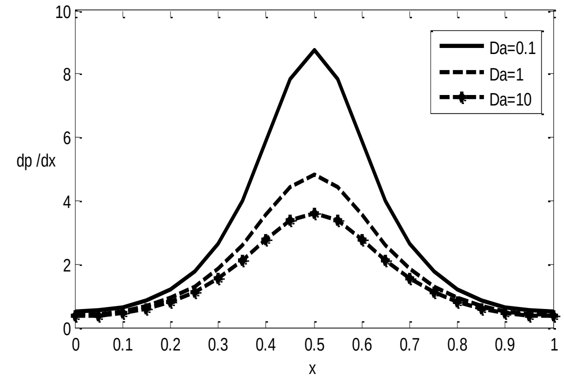

Fig. 3. The variation of axial pressure gradient $\frac{dp}{dx}$ for different values of Da.

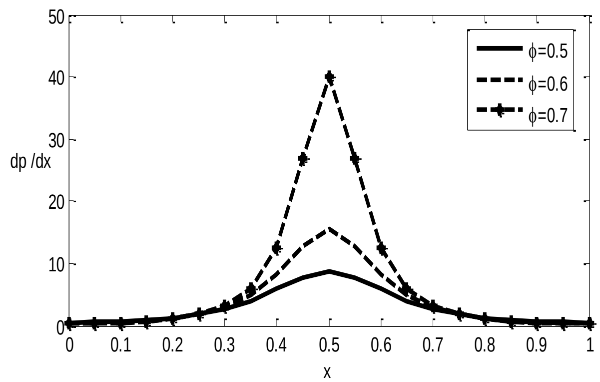

Fig. 4. The variation of axial pressure gradient $\frac{dp}{dx}$ for different values of ϕ.

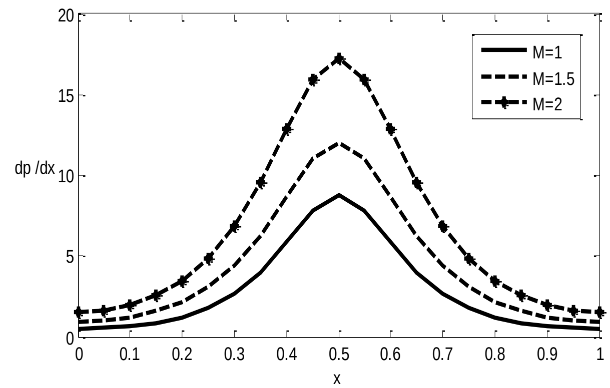

Fig. 5. The variation of axial pressure gradient $\frac{dp}{dx}$ for different values of M .

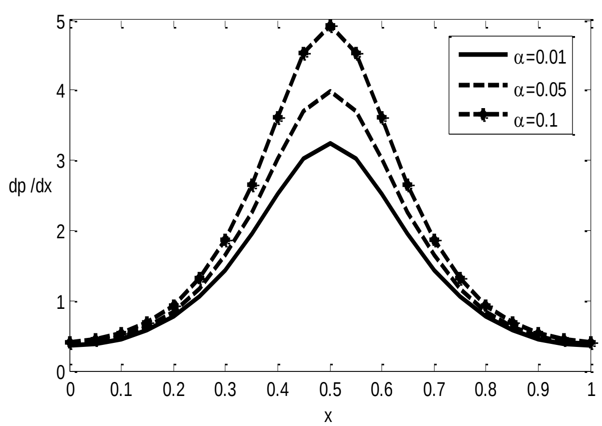

Fig. 6. The variation of axial pressure gradient $\frac{dp}{dx}$ for different values of α.

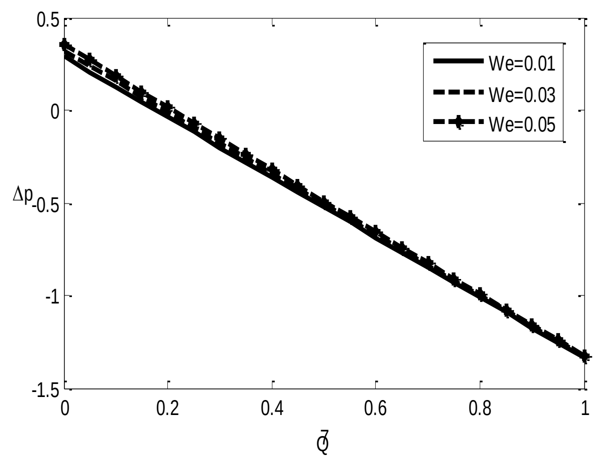

Fig. 7. The variation of pressure rise Δp for different values of We.

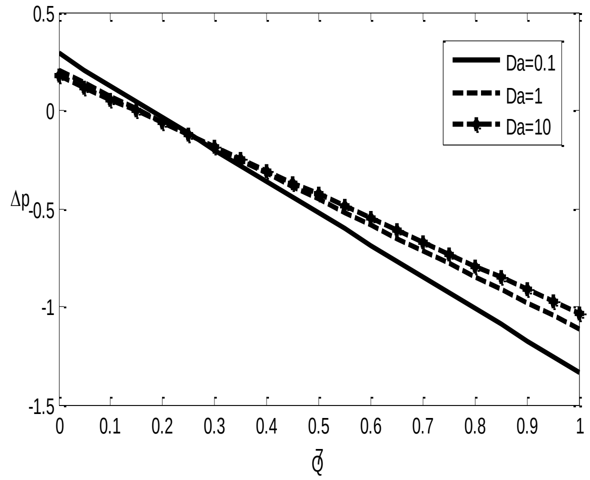

Fig. 8. The variation of pressure rise Δp for different values of Da.

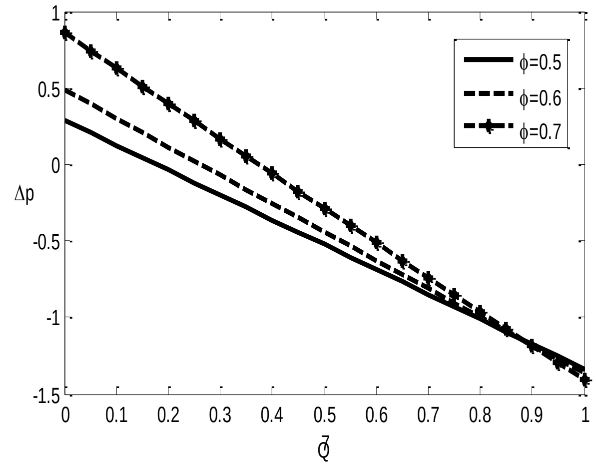

Fig. 9. The variation of pressure rise Δp for different values of ϕ.

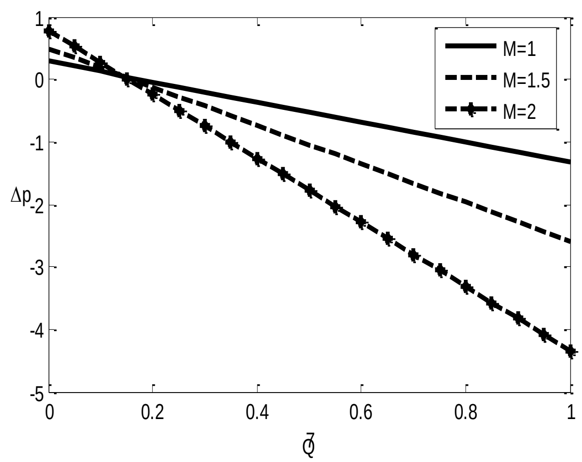

Fig. 10. The variation of pressure rise Δp for different values of M .

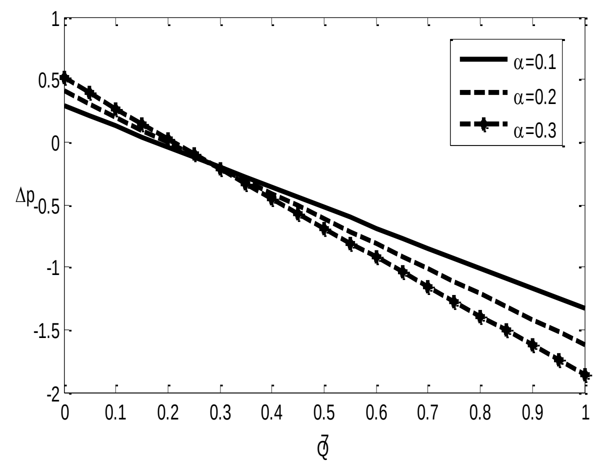

Fig. 11. The variation of pressure rise Δp for different values of α .

CONFLICT OF INTERESTS

The authors declare that there is no conflict of interests.

REFERENCES

[1] W. Bayliss, E. Starling, The mechanism of pancreatic secretion, J. Physiol. 28 (1902), 325-52.

[2] J.C. Burns, J. Parkes, Peristaltic motion, J. Fluid Mech. 29 (1967) 731–743.

[3] Y.C. Fung, C.S. Yih, Peristaltic transport, J. Appl. Mech. (1968) 901–905.

[4] T. Hayat, Y. Wang, A.M. Siddiqui, K. Hutter, Peristaltic motion of a Johnson–Segalman fluid in a planar channel, Math. Probl. Eng. 2003 (2003), 1–23.

[5] T. Hayat, Y. Wang, K. Hutter, S. Asghar, M. Siddiqui, Peristaltic transport of an oldroyd-B fluid in a planar channel, Math. Probl. Eng. 2004 (2004) 347–376.

[6] T. Hayat, N. Ali, Peristaltically induced motion of a MHD third grade fluid in a deformable tube, Physica A, Stat. Mech. Appl. 370 (2006) 225–239.

[7] T.D. Brown, T.K. Hung, Computational and experimental investigations of two dimensional non-linear peristaltic flows, J. Fluid Mech. 83 (1977), 249–272.

[8] S. Takabatake, K. Ayukawa, A. Mori, A peristaltic pumping in cylindrical tubes: a numerical study of fluid transport and its efficiency, J. Fluid Mech. 147 (1988) 267–283.

[9] Suripeddi Srinivas, N.Ch.P. Ramacharyulu, Peristaltic transport of a viscoelastic fluid (a long wavelength approximation), Arch. Mech. 47 (1995) 1157–1167.

[10] O. Eytan, D. Elad, Analysis of intra-uterine fluid motion induced by uterine contractions, Bull. Math. Biol. 61 (1999) 221–238.

[11] C. Pozrikidis, A study of peristaltic flow, J. Fluid Mech. 180 (1987) 515–527.

[12] M.H. Haroun, Effect of wall compliance on peristaltic transport of a Newtonian fluid in an asymmetric channel, Math. Probl. Eng. 2006 (2006), Article ID 61475.

[13] V.K. Stud, G.S. Sephon, R.K. Mishra, Pumping action on blood flow by a magnetic field, Bull. Math. Biol. 39 (1977) 385–390.

[14] G. Radhakrishnamacharya, V. Radhakrishna Murthy, Heat transfer to peristaltic transport in a non-uniform channel, Def. Sci. J. 43 (1993) 275–280.

[15] T.W. Latham, Fluid motion in Peristaltic Pump, M.S. Thesis, MIII, Cambridge, Mass, 1966.

[16] M. Y. Jaffrin and A. H. Shapiro, Peristaltic Pumping, Ann. Rev. Fluid Mech. 3 (1971), 13-37.

[17] K.Vajravelu, G. Radhakrishnamacharya, and V. Radhakrishnamurty, Peristaltic flow and heat transfer in a vertical porous annulus with long wave approximation. Int J. Nonlinear Mech. 42(2007), 754 – 759.

[18] K.Vajravelu, S. Sreenadh, , P. Lakshminarayana, , G. Sucharitha, and M. M. Rashidi, Peristaltic flow of phan-thien-tanner fluid in an asymmetric channel with porous medium, J. Appl. Fluid Mech. 9 (4) (2016), 1615-1625.

[19] M.V. Subba Reddy, A. Ramachandra Rao, and S. Sreenadh, Peristaltic motion of a power law fluid in an asymmetric channel, Int. J. Non-Linear Mech. 42 (2007), 1153 -1161.

[20] K. Vajravelu, S. Sreenadh, R. Hemadri Reddy, K. Murugeshan, Peristaltic Transport of a Casson fluid in contact with a Newtonian Fluid in a Circular Tube with permeable wall, Int. J. Fluid Mech. Res. 36 (3) (2009), 244-254.

[21] K. Vajravelu, S. Sreenadh, R. Saravana, Combined influence of velocity slip, temperature and concentration jump conditions on MHD peristaltic transport of a Carreau fluid in a non- uniform channel, Appl. Math. Comput. 225 (2013), 656-676.

[22] K. Vajravelu, S. Sreenadh, P. Lakshminarayana G. Sucharitha, The effect of heat transfer on the nonlinear peristaltic transport of a Jeffrey fluid through a finite vertical porous channel, Int. J. Biomath. 7(2) (2016), 1650023.

[23] E.F. El Shehawey, A.M.F. Sobh, and E.M.E. Elbarbary, Peristaltic motion of a generalized Newtonian fluid through a porous medium, J. Phys. Soc. Japan, 69 (2000), 401-407.

[24] N.A.S. Afifi and N.S. Gad, Interaction of peristaltic flow with pulsatile magneto fluid through a porous medium, Acta Mech. 149 (2001), 229-237.

[25] Kh.S. Mekheimer and T.H. Al-Arabi, Nonlinear peristaltic transport of MHD flow through a porous medium, Int. J. Math. Math. Sci. 26 (2003), 1663-1682.

[26] E.F. El Shehawey, N.T. Eldabe, E.M. Elghazy, and A. Ebaid, peristaltic transport in an asymmetric channel through a porous medium, Appl. Math. Comput. 182 (2006), 140-150.

[27] S. Navaneeswara Reddy and G. Viswanatha Reddy, Slip effects on peristaltic motion of a williamson fluid through a porous medium in a planar channel, Asian J. Current Eng. Math. 2 (1) (2013), 53 – 58.

[28] A. M. Abdulhadi and T. S. Ahmed, Effect of magnetic field on peristaltic flow of Williamson fluid through a porous medium in an inclined tapered asymmetric channel, Math. Theory Model. 7 (2017), 549-65.

[29] M. Mishra and A. Ramachandra Rao, Peristaltic transport of a Newtonian fluid in an asymmetric channel, Z. Angew. Math. Phys. (ZAMP), 54 (2003), 532-550.

[30] N. Ali, Q. Hussain, T. Hayat and S. Asghar, Slip effects on the peristaltic transport of MHD fluid with variable viscosity, Phys. Lett. A, 372 (2008), 1477 -1489.